Spectral signatures of the Luttinger liquid to the charge-density-wave transition

M. Hohenadler,[1,*] G. Wellein,[2] A. R. Bishop,[3] A. Alvermann,[4] and H. Fehske[4]
[1]*Institute for Theoretical and Computational Physics, Graz University of Technology, 8010 Graz, Austria*
[2]*Computing Center, University Erlangen, 91058 Erlangen, Germany*
[3]*Theoretical Division and Center for Nonlinear Studies, Los Alamos National Laboratory, Los Alamos, New Mexico 87545, USA*
[4]*Institute for Physics, Ernst-Moritz-Arndt University Greifswald, 17487 Greifswald, Germany*
(Received 5 May 2006; published 30 June 2006)

Electron- and phonon spectral functions of the one-dimensional, spinless-fermion Holstein model at half filling are calculated in the four distinct regimes of the phase diagram, corresponding to an attractive or repulsive Luttinger liquid at weak electron-phonon coupling, and a band- or polaronic insulator at strong coupling. The results obtained by means of kernel polynomial and systematic cluster approaches reveal substantially different physics in these regimes and further indicate that the size of the phonon frequency significantly affects the nature of the quantum Peierls phase transition, the latter being either of the soft-mode or central-peak type. The generic features observed are relevant to several classes of low-dimensional materials.

DOI: 10.1103/PhysRevB.73.245120 PACS number(s): 71.10.Fd, 71.10.Hf, 71.30.+h, 71.45.Lr

I. INTRODUCTION

Low-dimensional materials like halogen-bridged transition metal complexes, ferroelectric perovskites, conjugated polymers, or organic charge-transfer salts are very susceptible to structural distortions driven by electron-phonon (EP) interaction. At commensurate band fillings these systems might undergo a Peierls or charge-density-wave (CDW) instability accompanied by a dimerization of the lattice but, unlike in conventional metals, both quantum lattice fluctuations and strong electronic correlations are important.[1] The challenge of understanding the related metal-insulator transition, especially in the strong-EP coupling regime and in conjunction with strong electronic correlations, has renewed the interest in models of interacting electrons and phonons.[2–5]

In this work, we compare in detail the spectral signatures of four physically distinct regimes in the phase diagram of the one-dimensional (1D) Holstein model of spinless fermions (HMSF) (Fig. 1). To this end, we calculate the single-particle spectral functions of electrons and phonons, using exact diagonalization (ED) in combination with cluster perturbation theory (CPT)[6] and the kernel polynomial method (KPM).[7] Besides the influence of the degree of phonon retardation on the nature of the Peierls transition, the wave-number dependence of the spectral functions missed in previous dynamical mean-field theory studies[3] turns out to be crucial for the 1D case considered here.

The paper is organized as follows. The model is introduced and its phase diagram reviewed in Sec. II. In Sec. III we present the methods used, and results are discussed in Sec. IV. Finally, we summarize in Sec. V.

II. MODEL

The Hamiltonian of the 1D HMSF

$$H = -t\sum_{\langle i,j\rangle} c_i^\dagger c_j + \omega_0 \sum_i b_i^\dagger b_i - g\omega_0 \sum_i \hat{n}_i (b_i^\dagger + b_i) \qquad (1)$$

describes a number of interesting general phenomena, and is particularly rewarding to study because it exhibits at half filling, as the EP coupling increases, a zero-temperature quantum phase transition from a metallic Luttinger liquid (LL) to an insulating Peierls state. In Eq. (1), $c_i^\dagger$ ($b_i^\dagger$) creates an electron (dispersionless phonon of energy ω_0) at site i of a 1D lattice with N sites. The first term describes hopping processes ($\propto t$) between neighboring sites $\langle i,j\rangle$, the second term gives the elastic and kinetic lattice energy, and the third term accounts for the local coupling ($\propto g$) between the lattice displacement $\hat{x}_i = b_i^\dagger + b_i$ and the electron density $\hat{n}_i = c_i^\dagger c_i$, all in the limit of infinite onsite (Hubbard) Coulomb repulsion, i.e., the site occupation numbers are $n_i = 0, 1$. Important parameters to be used here are the adiabaticity ratio ω_0/t and the dimensionless coupling $\lambda = \varepsilon_p/2t$, where $\varepsilon_p = g^2\omega_0$ is the polaron binding energy.

Despite its simplicity, the HMSF is not exactly solvable and a wide range of analytical and numerical methods have

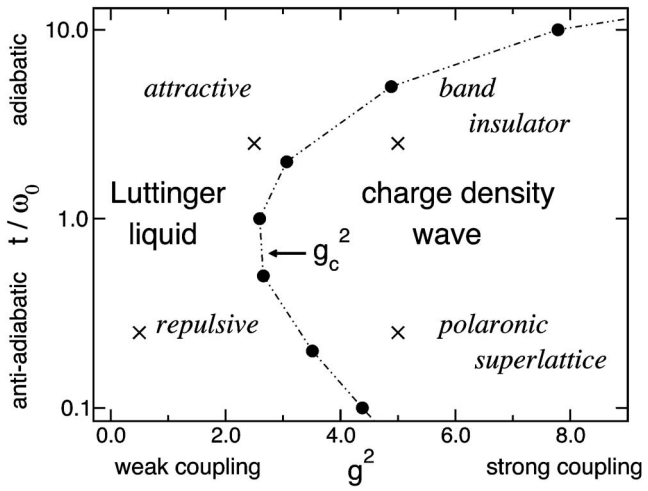

FIG. 1. DMRG ground-state phase diagram of the 1D half-filled HMSF (cf. Refs. 2 and 9). In the adiabatic limit $\omega_0 \to 0$ the critical dimensionless coupling constant λ_c converges to zero. For $\omega_0 > 0$, due to quantum phonon fluctuations, there exists a finite critical coupling $g_c(\omega_0)$. For $\omega_0 \to \infty$, the model exhibits a Kosterlitz-Thouless phase transition near $g_c^* = g_c(\omega_0 \to \infty)$.[2] Crosses indicate parameter sets used below.

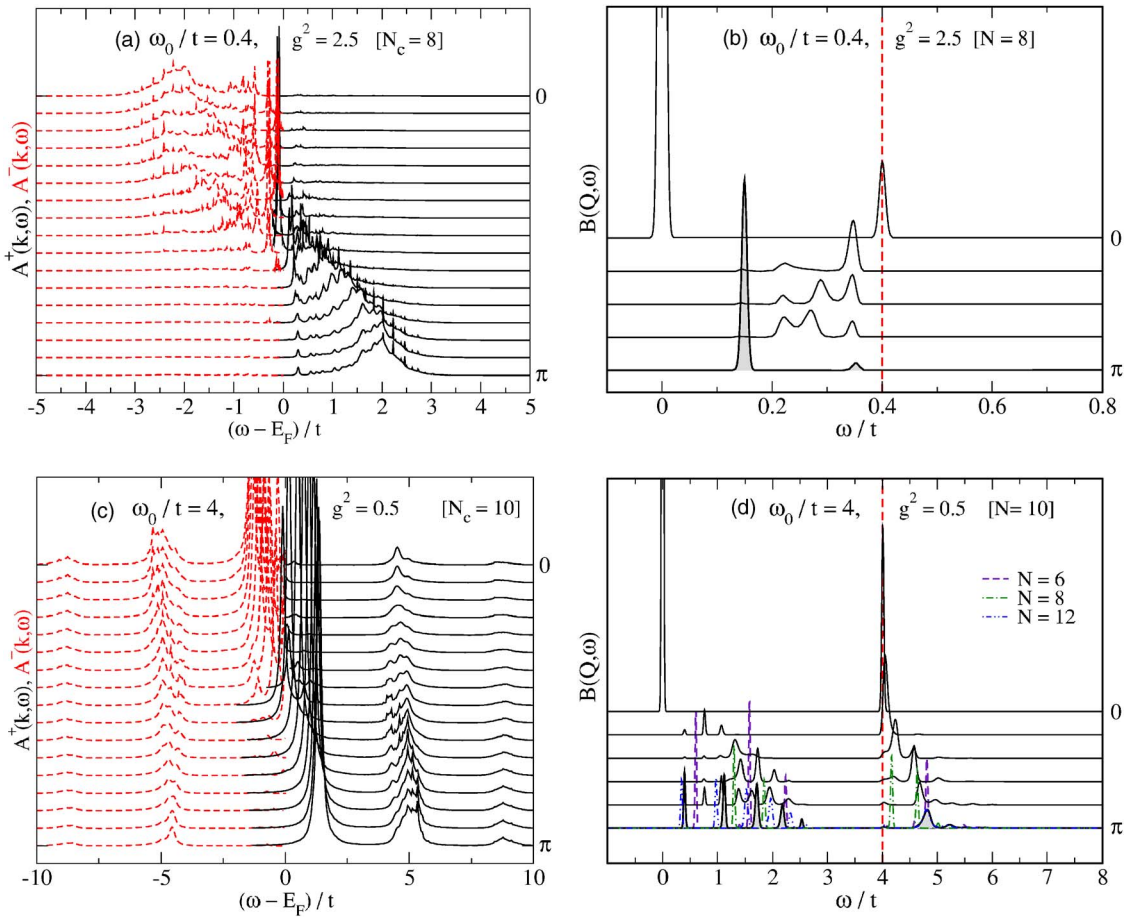

FIG. 2. (Color online) Left panel [(a), (c)]: Spectral density for photoemission $[A^-(k,\omega)$; red dashed lines] and inverse photoemission $[A^+(k,\omega)$; black solid lines] from CPT in the metallic LL phase. Energies are measured relative to the Fermi level E_F. Right panel [(b), (d)]: Corresponding exact phonon spectral function $B(Q,\omega)$ for the allowed wave numbers Q of N-site clusters. Electron and phonon spectra have been calculated in the adiabatic [attractive LL; (a), (b)] and antiadiabatic [repulsive LL; (c), (d)] weak-to-intermediate EP coupling regimes. Dashed vertical lines in (b), (d) indicate the bare phonon frequency.

been used to map out the ground-state phase diagram in the $g-\omega_0$ plane (see references in Ref. 8). At present the probably most precise phase boundary may be obtained by exact diagonalization and density matrix renormalization group (DMRG) techniques.[2,9] More recent large-scale DMRG calculations supplemented by a finite-size analysis have proved that at low (high) phonon frequencies the metallic LL phase is characterized by an attractive (repulsive) interaction.[10] But also above $g_c(\omega_0)$, where long-range CDW order sets in, there exist two physically distinct regimes, which can be classified, e.g., by their different optical response,[9] either as a band insulator in the adiabatic regime $\omega_0/t \ll 1$ or as a polaronic superlattice in the limit of large phonon frequencies $\omega_0/t \gg 1$ (see Fig. 1). Including the spin degrees of freedom and a finite Hubbard interaction allows for additional quantum phase transitions between Peierls and Mott insulating phases.[4] The half-filled HMSF captures the relevant physics of the more general quarter-filled Hubbard-Holstein model[3,4] in the regime of large Hubbard repulsion $U \gg t$, often realized in experiment, where onsite bipolaron formation is suppressed.

III. METHODS

The $T=0$ electron spectral function is related to the one-electron Green's function via

$$A(k,\omega) = -\frac{1}{\pi}\mathrm{Im}\, G(k,\omega) = A^+(k,\omega) + A^-(k,\omega), \qquad (2)$$

where

$$A^{\pm}(k,\omega) = -\frac{1}{\pi}\mathrm{Im}\lim_{\eta\to 0^+}\langle\psi_0|c_k^{\mp}\frac{1}{\omega + \mathrm{i}\,\eta \mp H}c_k^{\pm}|\psi_0\rangle, \qquad (3)$$

$c_k^- = c_k$, $c_k^+ = c_k^\dagger$, and $|\psi_0\rangle$ is the ground state of the HMSF with $N_e = N/2$ electrons. $A^-(k,\omega)$ $[A^+(k,\omega)]$ describes (inverse) photoemission of an (injected) electron with momentum k and energy ω.

Relying on approximation-free numerical approaches (here ED) we can calculate exact Green's functions for finite systems only. To obtain an approximation of $G(k,\omega)$ for the infinite lattice, we can exploit CPT.[6] To this end, we divide the infinite system into identical clusters of N_c sites each, and determine the electron cluster Green's function $G_{ij}^{(c)}(\omega)$ for

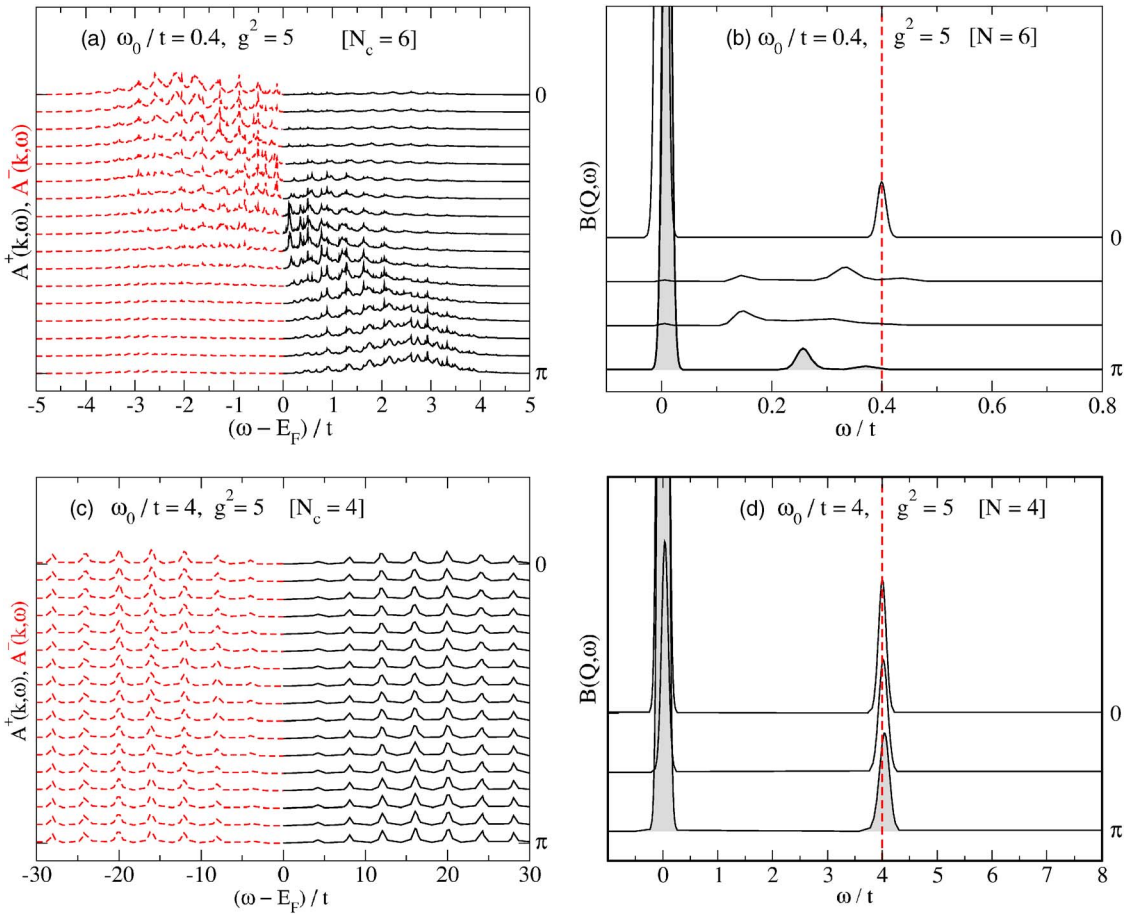

FIG. 3. (Color online) As in Fig. 2, but for parameters in the insulating CDW phase, and for the case of a band insulator [(a), (b)] and a polaronic superlattice [(c), (d)].

all nonequivalent pairs of sites $i,j=1,\ldots,N_c$ by the KPM (for details see Ref. 7). The phonon Hilbert space is truncated such that the resulting error of the spectra is negligible ($<10^{-4}$), and we have used 1024 Chebyshev moments. In a second step, the Green's function $G(k,\omega)$ for the infinite lattice is obtained from the first-order result[6]

$$\tilde{G}_{ij}(k,\omega)=\left[\frac{G^{(c)}(\omega)}{1-\tilde{t}(k)G^{(c)}(\omega)}\right]_{ij} \tag{4}$$

of a strong-coupling expansion in the intercluster hopping operator $\tilde{t}(k)$ as follows:

$$G(k,\omega)=\frac{1}{N_c}\sum_{i,j=1}^{N_c}\tilde{G}_{ij}(k,\omega)e^{-ik\cdot(r_i-r_j)}. \tag{5}$$

The $T=0$ phonon spectral function is defined as

$$B(q,\omega)=-\frac{1}{\pi}\,\mathrm{Im}\,D(q,\omega) \tag{6}$$

with

$$D(q,\omega)=\lim_{\eta\to 0^+}\langle\psi_0|\hat{x}_q\frac{1}{\omega+i\eta-H}\hat{x}_{-q}|\psi_0\rangle \tag{7}$$

for $\omega\geq 0$ and $\hat{x}_q=N^{-1/2}\Sigma_j\hat{x}_j e^{-ir_j\cdot q}$. For the HMSF (1), $B(q,\omega)$ is symmetric in q, and we have a dispersionless bare propagator $D_0(q,\omega)=2\omega_0/(\omega^2-\omega_0^2)$. The EP interaction will renormalize the phonon frequency, whereby $D(q,\omega)$ attains a q dependence. Concerning notation, we shall reserve the capital Q for allowed wave numbers of finite clusters.

IV. RESULTS

The crosses in the phase diagram (Fig. 1) mark the four parameter sets to be used in the sequel.

Figures 2(a) and 2(c) show results for the CPT electron spectral functions $A^{\pm}(k,\omega)$ in the *metallic region*. In the adiabatic (attractive LL) regime [Fig. 2(a)], we find a rather pronounced peak at the Fermi level E_F but nevertheless the system is not a Fermi liquid. The nonuniversal LL parameters (charge velocity and interaction coefficient) can be determined from a DMRG finite-size scaling.[10] At $k=k_F$, very little spectral weight is contained in the incoherent part of the spectrum. By contrast, away from the Fermi momentum, almost all of the spectral weight resides in the incoherent part, whose maximum follows quite closely the free dispersion

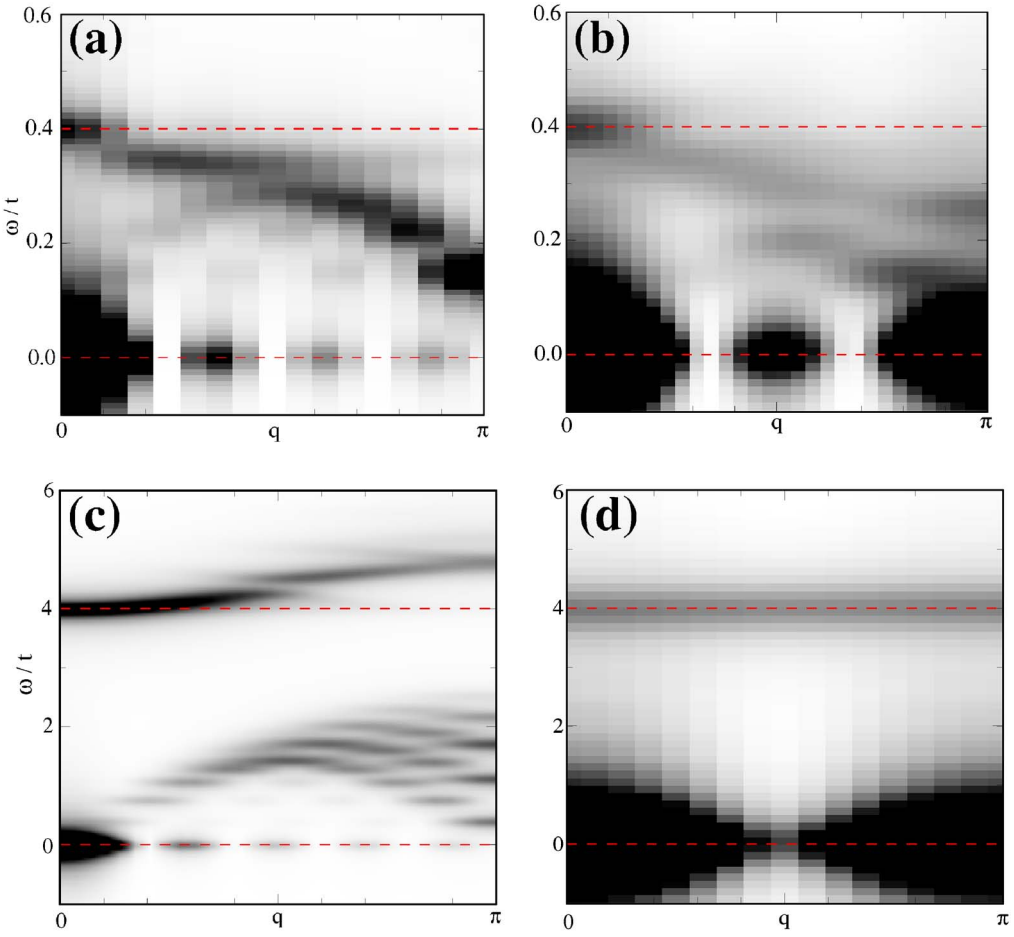

FIG. 4. (Color online) Density plots of the (CPT) phonon spectral function $B(q,\omega)$, where panels (a), (b), (c), and (d) correspond to the attractive LL ($\omega_0/t=0.4$, $g^2=2.5$), band insulator ($\omega_0/t=0.4$, $g^2=5$), repulsive LL ($\omega_0/t=4$, $g^2=0.5$), and polaron superlattice regimes ($\omega_0/t=4$, $g^2=5$), respectively.

$-2t\cos k$ [notice the symmetry of $A^-(k<k_F)$ and $A^+(k>k_F)$]. As these states are accessible only via (multi-) phonon excitations, the width of the incoherent band is proportional to g^2.

The spectrum in the antiadiabatic (repulsive LL) regime, Fig. 2(c), looks significantly different. Due to the larger coupling $\lambda=\varepsilon_p/2t=1$ (with respect to the bare electronic bandwidth), as compared to $\lambda=0.5$ in Fig. 2(a), the carriers are more strongly renormalized. This is reflected in the reduced bandwidth $W\approx 3t$, with the spectral weight being more evenly distributed than in the adiabatic case. The fact that $\omega_0>W$ gives rise to multiple, nondispersive sidebands at energies $E_F\pm n\omega_0$.

In Figs. 2(b) and 2(d) we present the corresponding phonon spectral functions, as obtained from ED. Again we find pronounced differences between the adiabatic [Fig. 2(b)] and the antiadiabatic [Fig. 2(d)] cases, revealing the distinct nature of the Peierls instability—driven by the EP coupling λ or g—for small and large ω_0/t.

For $\omega_0/t=0.4$ [Fig. 2(c)], we observe a peak at $\omega=0$ originating from the homogeneous ($Q=0$) shift of the electronic level for $\lambda>0$, as well as a signal located at the bare phonon energy ω_0. More importantly, the phonon excitations gradually soften near the zone boundary ($Q=\pi$) already in the LL phase, a behavior characteristic of the Peierls transition traditionally regarded as a displacive phase transition.

For large ω_0/t [Fig. 2(d)], we observe two main absorption features. The first excitation near ω_0 becomes even harder with increasing wave number, in contrast to the phonon softening in the adiabatic regime. The second branch emerging from $\omega=0$ ($Q=0$) resembles the two-spinon continuum[11] of the XXZ model (onto which the spinless Holstein model may be mapped in the antiadiabatic strong-coupling limit[2]), i.e., it can be traced back to phonon signatures of the corresponding electronic excitations.

We now turn to the *insulating state* of the HMSF (Fig. 3). Due to the Peierls distortion, and the formation of long-range CDW order for $N\to\infty$, a gap opens at E_F. In the adiabatic regime, the transition is from a LL to a traditional Peierls band insulator, whereas in the antiadiabatic regime, the charge carriers first undergo a crossover to small polarons (polaronic metal), which then (upon increasing the coupling further) order to form a polaronic superlattice.

From Fig. 3(a) we see that the gap in the single-particle spectrum is still quite small. This is partly due to the fact that CPT in the form used here does not fully take into account long-range order. At k_F, the strongest signatures lie just above and below E_F, with the incoherent part again being

very small. Away from k_F, the incoherent band is significantly broadened (again almost $\propto g^2$ at $k=\pi$), and reflects the Poisson distribution of the phonons in the ground state. Nevertheless, we can still detect the dispersion of the split electronic band.

In contrast to the adiabatic case of Fig. 3(a), Fig. 3(c) shows a clear gap for all k. The polaronic charge carriers—in addition to forming a superlattice—are quasilocalized, leading to dispersionless excitations near energies $E_F \pm n\omega_0$.

The phonon spectra for the insulating phase are shown in Figs. 3(b) and 3(d). In the adiabatic case of Fig. 3(b), the zone boundary phonon has almost completely softened. In the limit $N\to\infty$, we expect a perfect degeneracy of $Q=0,\pi$ for $g>g_c$, and a macroscopic population of the soft phonon mode. For $\omega_0/t=4$ [Fig. 3(d)], there exist two completely flat signatures at $\omega=0$ and $\omega=\omega_0$ [cf. Fig. 4(d)], the former having very large spectral weight due to the large "phonon content" of the polaron band.

Similar to the results for $A(k,\omega)$, it is desirable to obtain results for the phonon spectrum of the infinite system. However, in deriving a CPT-like approach to the phonon Green's function $D(q,\omega)$, it turns out that the first-order correction in $\tilde{t}$ vanishes identically, since the electron number per cluster is a conserved quantity. Therefore, CPT results in a simple Fourier transformation of the cluster Green's function (again obtained by the KPM),

$$D(q,\omega)=\frac{1}{N_c}\sum_{i,j=1}^{N_c} D_{ij}^{(c)}(\omega)e^{-iq\cdot(r_i-r_j)}. \tag{8}$$

Notice that this result still becomes exact for the free Green's function $D_0(q,\omega)$, and in the limit of strong coupling and large phonon frequency, when t is a small parameter. As the calculation of the second-order contribution is extremely demanding we have restricted ourselves to this expansion to illustrate the q dependence of $B(q,\omega)$ in Fig. 4.

The density plots in Fig. 4 clearly summarize the differences between the adiabatic and antiadiabatic regimes, and between the LL and CDW phases of the HMSF. In Fig. 4(a) we see the renormalized phonon dispersion (q), which softens with increasing EP coupling, leading to a degeneracy of excitations at $Q=0,\pi$ at g_c [see panel (b)]. The strong zero-energy absorption feature at $\pi/2$ is an artifact of the small cluster size and the open boundary conditions used in the CPT scheme [cf. Fig. 3(b)]. Above the Peierls transition we find—in agreement with recent Monte Carlo simulations[5]—that the soft $Q=\pi$ phonon mode splits into two branches with the upper one hardening as the EP coupling increases further.

Quite differently, in the antiadiabatic case, we observe two phonon signatures for all $g>0$. In the LL phase the bare phonon mode hardens, whereas a second mode becomes strongly over damped near $Q=\pi$ [Fig. 4(c)]. Finally, Fig. 4(d) reveals a dispersionless signal at $\omega=\omega_0$, as well as the flat polaron band at $\omega\approx 0$ for the polaronic CDW state. Thus, with increasing phonon frequency, we find a crossover from a soft-mode (displacive) to a central-peak-like (order-disorder-type) phase transition, similar to the analysis of the spin-Peierls transition motivated by $CuGeO_3$.[9]

V. SUMMARY

By presenting highly reliable numerical results for the electron- and phonon-spectral function, we have identified four physically distinct regions in the phase diagram of the one-dimensional spinless Holstein model, characterized by important generic features such as attractive or repulsive Luttinger liquid behavior and phonon softening, which are highly relevant for low-dimensional condensed matter systems.

Note added in proof. The results presented for the phonon spectral function have recently been confirmed by means of analytical calculations by Sykora *et al.*.[12]

ACKNOWLEDGMENTS

This work was supported by the FWF Project No. P15834, the DFG through Contract No. SPP1073, KONWIHR, and HPC Europa. Work at Los Alamos is performed under the auspices of USDOE. We would like to thank M. Aichhorn, E. Jeckelmann, J. Loos, and A. Weiße for useful discussions, and acknowledge generous computer time granted by the HLRN Berlin, LRZ Munich, and HLR Stuttgart.

*Electronic address: hohenadler@itp.tu-graz.ac.at

[1] N. Tsuda, K. Nasu, A. Yanese, and K. Siratori, *Electronic Conduction in Oxides* (Springer-Verlag, Berlin, 1990); A. R. Bishop and B. I. Swanson, Los Alamos Sci. **21**, 133 (1993).

[2] R. J. Bursill, R. H. McKenzie, and C. J. Hamer, Phys. Rev. Lett. **80**, 5607 (1998); A. Weiße and H. Fehske, Phys. Rev. B **58**, 13526 (1998); E. Jeckelmann, C. Zhang, and S. R. White, *ibid.* **60**, 7950 (1999).

[3] D. Meyer, A. C. Hewson, and R. Bulla, Phys. Rev. Lett. **89**, 196401 (2002); M. Capone and S. Ciuchi, *ibid.* **91**, 186405 (2003); P. Paci, M. Capone, E. Cappelluti, S. Ciuchi, C. Grimaldi, and L. Pietronero, *ibid.* **94**, 036406 (2005); G. Sangiovanni, M. Capone, C. Castellani, and M. Grilli, *ibid.* **94**, 026401 (2005); W. Koller, A. C. Hewson, and D. M. Edwards, Phys. Rev. Lett. **95**, 256401 (2005).

[4] R. T. Clay and R. P. Hardikar, Phys. Rev. Lett. **95**, 096401 (2005); H. Matsueda, T. Tohyama, and S. Maekawa, cond-mat/0511068 (unpublished); W. Q. Ning, H. Zhao, C. Q. Wu, and H. Q. Lin, Phys. Rev. Lett. **96**, 156402 (2006); M. Tezuka, R. Arita, and H. Aoki, *ibid.* **95**, 226401 (2005); H. Fehske, G. Wellein, G. Hager, A. Weiße, and A. R. Bishop, Phys. Rev. B **69**, 165115 (2004).

[5] C. E. Creffield, G. Sangiovanni, and M. Capone, Eur. Phys. J. B **44**, 175 (2005).

[6] D. Sénéchal, D. Perez, and D. Plouffe, Phys. Rev. B **66**, 075129 (2002); M. Hohenadler, M. Aichhorn, and W. von der Linden,

Phys. Rev. B **68**, 184304 (2003).
[7] A. Weiße, G. Wellein, A. Alvermann, and H. Fehske, Rev. Mod. Phys. **78**, 275 (2006).
[8] S. Sykora, A. Hübsch, K. W. Becker, G. Wellein, and H. Fehske, Phys. Rev. B **71**, 045112 (2005); S. Sykora, A. Hübsch, and K. W. Becker, Eur. Phys. J. B **51**, 181 (2006).
[9] H. Fehske, M. Holicki, and A. Weiße, in Adv. Solid State Phys. **40**, 235 (2000); G. Wellein, H. Fehske, and A. P. Kampf, Phys. Rev. Lett. **81**, 3956 (1998).
[10] H. Fehske, G. Wellein, G. Hager, A. Weiße, K. W. Becker, and A. R. Bishop, Physica B **359-361**, 699 (2005).
[11] L. D. Fadeev and L. A. Takhtajan, Phys. Lett. **85A**, 375 (1981); M. Mohan and G. Muller, Phys. Rev. B **27**, 1776 (1983).
[12] S. Sykora, A. Huebsch, and K. W. Becker, cond-mat/0605643 (unpublished).